



Optimization of high-throughput lipid screening of the microalga *Nannochloropsis oceanica* using BODIPY 505/515

Christian Südfeld^{a,*}, Michal Hubáček^a, Sarah D'Adamo^a, René H. Wijffels^{a,b},
Maria J. Barbosa^{a,c}

^a Wageningen University, Bioprocess Engineering, PO Box 16, 6700 AA Wageningen, Netherlands

^b Faculty of Biosciences and Aquaculture, Nord University, N-8049 Bode, Norway

^c Department of Biology, University of Bergen, PO Box 7803, 5006 Bergen, Norway

ARTICLE INFO

Keywords:

Microalgae
Nannochloropsis
Neutral lipid staining
BODIPY
Flow cytometry
Viability

ABSTRACT

Background: Microalgae are considered a promising platform for sustainable lipid production. Despite this, productivities need to be improved to facilitate an economically viable production process. This can be achieved through strain improvement, for instance by genetic engineering. Strain improvement strategies often deploy high-throughput screening platforms i.a. involving single-cell methodologies such as fluorescence-activated cell sorting (FACS) for the identification and isolation of better-performing strains. The heterokont microalga *Nannochloropsis* is a prospective candidate for the industrial production of lipids. Previous studies have reported the isolation of high lipid-producing *Nannochloropsis* strains by combining qualitative staining of lipid bodies using the fluorophoric dye BODIPY with FACS methodology. However, it has never been investigated how cellular physiology and different staining conditions hamper the reproducibility of this method as a quantitative screening procedure.

Results: Here we report the development of an optimized single cell lipid screening procedure for *Nannochloropsis oceanica*. Systematic assessment of different staining conditions revealed that treatment with 6% DMSO and 1.2 $\mu\text{g ml}^{-1}$ BODIPY for 15 min is ideal for staining neutral lipids in an exponentially growing culture of *N. oceanica*. Cultures that are overproducing lipids, for example after exposure to external stimuli such as nutrient deprivation stress, require treatment with 10% DMSO and 1.2–1.6 $\mu\text{g ml}^{-1}$ BODIPY for 36 min to facilitate complete staining of lipid bodies. We verify that DMSO is required to permeabilize the particularly tough cell barrier of *Nannochloropsis* and we show that exposure to 10% DMSO does not affect cell viability. Increasing concentrations of BODIPY, however, correlated with a decrease in viability when screening stressed cultures. Using the optimized protocol, reproductive viabilities can be expected to be ~91% and 83–82% for non-stressed and stressed cultures respectively. The optimized procedure allows for a quantitative prediction of cellular neutral lipids ($R^2 = 0.981$), as determined by comparison to results obtained through a reference procedure.

1. Introduction

Oleaginous microalgae are widely considered to be a promising platform for the production of commercially interesting lipids and biofuel feedstocks due to their ability to grow photoautotrophically with relatively high biomass productivities on non-arable soil [1,2]. Some species accumulate considerable amounts of triacylglycerides (TAGs) as an energy storage compound in subcellular structures called lipid bodies [3]. Energy-rich TAGs are readily transesterified into fatty acid methyl esters (FAMES), which are suitable feedstocks for biofuel products [4]. In

particular, the heterokont *Nannochloropsis* is emerging as a model genus for industrial lipid production [5,6] due to robust growth and biodiesel-suitable fatty acid compositions [6–9]. In a comparative study with 9 different *Nannochloropsis* strains, *N. oceanica* was found to be the best candidate for biofuel production processes [10]. Although the projections for areal lipid productivities are promising, microalgae-derived biofuel feedstocks have yet to reach economic feasibility [11]. One way to increase productivities and reduce costs is to find better-performing species. This could be achieved through bioprospecting or strain improvement techniques, such as genetic engineering, adaptive

* Corresponding author.

E-mail address: christian.sudfeld@wur.nl (C. Südfeld).

<https://doi.org/10.1016/j.algal.2020.102138>

Received 15 June 2020; Received in revised form 13 November 2020; Accepted 13 November 2020

Available online 21 November 2020

2211-9264/© 2020 The Authors. Published by Elsevier B.V. This is an open access article under the CC BY license (<http://creativecommons.org/licenses/by/4.0/>).

laboratory evolution or random mutagenesis. All of these strategies frequently deploy high-throughput screening procedures and single cell methodologies such as fluorescence-activated cell sorting (FACS) have gained an outstanding importance in the field [12,13].

The emergence of high-throughput screening platforms for the isolation of microalgal strains is accompanied by a need for methods to quantify lipids in single cells in order to allow identification of strains with superior TAG contents. Fluorophore dyes are a useful tool for this purpose because they facilitate cellular imaging for a variety of compounds *in vivo* and allow selection of interesting traits in combination with FACS [13,14]. Lipid bodies were first visualized using fluorescence microscopy and flow cytometry by staining mammalian cells with Nile Red [15], and since then, this dye is among the most commonly employed lipophilic fluorophores [16]. The molecule from the benzo[*a*]phenoxazine family has several desirable properties such as a high quantum yield, intense brightness, low background fluorescence in aqueous solutions and a wide solvatochromic range, which permits discrimination between fluorescence emitted by molecules dissolved in either neutral or polar lipids [17]. More recently, other fluorophores have been discovered that are advantageous for several purposes such as specifically staining neutral and not polar lipids. Among these are BODIPY dyes [18,19], cyanine dyes [20], monodansylpentane [21,22], thalidomide analogs [23,24] and the benzothiadiazole derivative CBD-Fluor [25,26]. Some of these fluorophores have desirable properties in specificity for TAGs, cell penetration, higher signal intensities and improved resistance to photobleaching. Although none of them are as widely employed as Nile Red, considerable research has been devoted to understanding and utilizing BODIPY derivatives. Because this group of dyes has shown promising results for quantifying TAGs in different types of cells including microalgae [19,27,28], we here focus on BODIPY. BODIPY is usually dissolved in an organic solvent such as acetone or dimethyl sulfoxide (DMSO). In some cases the solvent is not only required for dissolving the molecule but further to ensure dye delivery by facilitating cell permeation. It was previously demonstrated that some microalgal species will not take up fluorophores unless they are permeabilized through appropriate pretreatments such as exposure to glycerol or DMSO [29]. BODIPY staining procedures for microalgae almost exclusively rely on DMSO for dissolving and delivery of the dye whereas other solvents play a tangential role [28].

The green fluorescing derivative BODIPY 505/515 has received reasonable attention as a dye for imaging lipid droplets in *Nannochloropsis* and it is applied for flow cytometric high-throughput screening and cell sorting [30,31]. Unfortunately, staining protocols that allow an accurate and reproducible quantitation of cellular TAG contents are lacking for this genus because research is hampered by the low permeability of the cell barrier of *Nannochloropsis* for dyes [29,32,33]. Previous studies have shown that exposure of cells to varying concentrations of DMSO greatly influences BODIPY uptake [29], suggesting that solvent concentration plays a key role for dye delivery. Strain improvement of this genus by high-throughput screening procedures would be significantly improved by the availability of optimized staining protocols that result in a complete and quantifiable staining of lipids. For the isolation of improved strains via cell sorting it is furthermore of paramount importance that sorted cells maintain reproductive viability [34]. It was previously shown that DMSO can be toxic to *Nannochloropsis* at high concentrations and that staining *Nannochloropsis* with Nile Red in conjunction with FACS affects cell viability [35]. However, no studies have systematically addressed the impact of BODIPY staining and FACS on cell viability of *Nannochloropsis*. A staining protocol featuring low cytotoxicity and quantitative prediction of single cell lipid contents would lay the foundation for the isolation of lipid-rich *Nannochloropsis* strains by high-throughput methodologies.

Previous studies on *Chlamydomonas* have shown that the isolation of lipid-rich strains is possible by screening mutant libraries specifically after the application of environmental stress such as nitrogen (N)

deprivation [36]. This approach is likely also a viable choice for screening other microalgal species for strains with elevated lipid contents because high levels of TAG accumulation are generally only observed in microalgae that have experienced nutrient stress [37–40]. Specifically *Nannochloropsis* shows profound rearrangements of metabolic processes in response to N stress that are not limited to lipid accumulation but include a plurality of physiological changes such as an overhaul of the photosynthetic apparatus and thickening of the cell wall [41–46]. However, no reports exist on the repercussions of these physiological and structural alterations on the applicability of BODIPY staining procedures or on cell viability after sorting. An improved *Nannochloropsis* lipid staining protocol might need to take cellular physiology into account in order to safeguard universal applicability for cultures grown under any cultivation condition.

The aim of our study was to develop an optimized BODIPY staining procedure for *N. oceanica* cells that would be suitable for direct application in high-throughput screening and sorting. By investigating the effect of DMSO treatment and BODIPY concentration on dye uptake in *N. oceanica* cells grown under replete and N-depleted conditions we wanted to ensure that this method would be adequately staining cells regardless of their physiological state. Lastly we wanted to minimize the amount of stress that this staining procedure would cause to an algal cell, by testing the effect of staining on cell viability, also in conjunction with stress induced by cell sorting.

2. Materials and methods

2.1. Media and strains

N. oceanica IMET1 was a kind gift from prof. Jian Xu (Qingdao Institute for Bioenergy and Bioprocess Technology, Chinese Academy of Sciences). The microalga was cultivated in artificial sea water (ASW) containing 419.23 mM NaCl, 22.53 mM Na₂SO₄, 5.42 mM CaCl₂, 4.88 mM K₂SO₄, 48.21 mM MgCl₂ and 20 mM HEPES at pH 8, supplemented with 2 ml l⁻¹ of commercial nutribloom plus (Necton, Portugal) growth media (ASW-NB) in an HT Multitron Pro (Infors Benelux, Netherlands) orbital shaker unit that was operated at 25 °C and 90 rpm shaking frequency with 0.2% CO₂-enriched air under warm-white fluorescent light bulbs at an intensity of 150 μmol m⁻² s⁻¹ with a 16:8 h diurnal cycle. For experiments with stressed cultures, ASW was supplemented with 2 ml l⁻¹ of a modified version of nutribloom plus that was lacking NaNO₃ (ASW-NB-N).

For cultivation on solid medium, ASW was supplemented with 1% (*w/v*) of agar (Merck) before autoclaving, cooled to 60 °C and mixed with 2 ml l⁻¹ of nutribloom plus before distribution into single-well plates for solidification. Algae-containing plates were incubated at 25 °C in ambient air under warm-white fluorescent light bulbs at an intensity of 80 μmol m⁻² s⁻¹ with a 16:8 h diurnal cycle.

2.2. Flow cytometry analysis

BODIPY fluorescence emission was quantified by flow cytometry analysis on an SH800S (Sony Biotechnology, USA) cell sorter instrument equipped with a 70 μm nozzle microfluidic chip and a 488 nm laser, unless noted otherwise. Detector wavelengths for different channels were: 488 nm (forward scatter, gain 2); 488 nm (side scatter, gain 22%); 510 ± 10 nm (BODIPY, gain 29%); 720 ± 30 nm (chlorophyll *a* autofluorescence, gain 40%). For standard fluorescence analyses a minimum of 100,000 events were screened per sample. Gating was applied according to supplementary Fig. S1 to remove background noise using an automated gating pipeline written in R statistical computing software [47] configured with the flowcore [48], flowWorkspace [49] and gcyto [50] packages of the Bioconductor project [51]. Density curves in Figs. 1, 2 and S3 are smoothed kernel density estimates that were computed by Gaussian approximation with the standard kernel and bandwidth parameters provided in the basic R stats package [47].

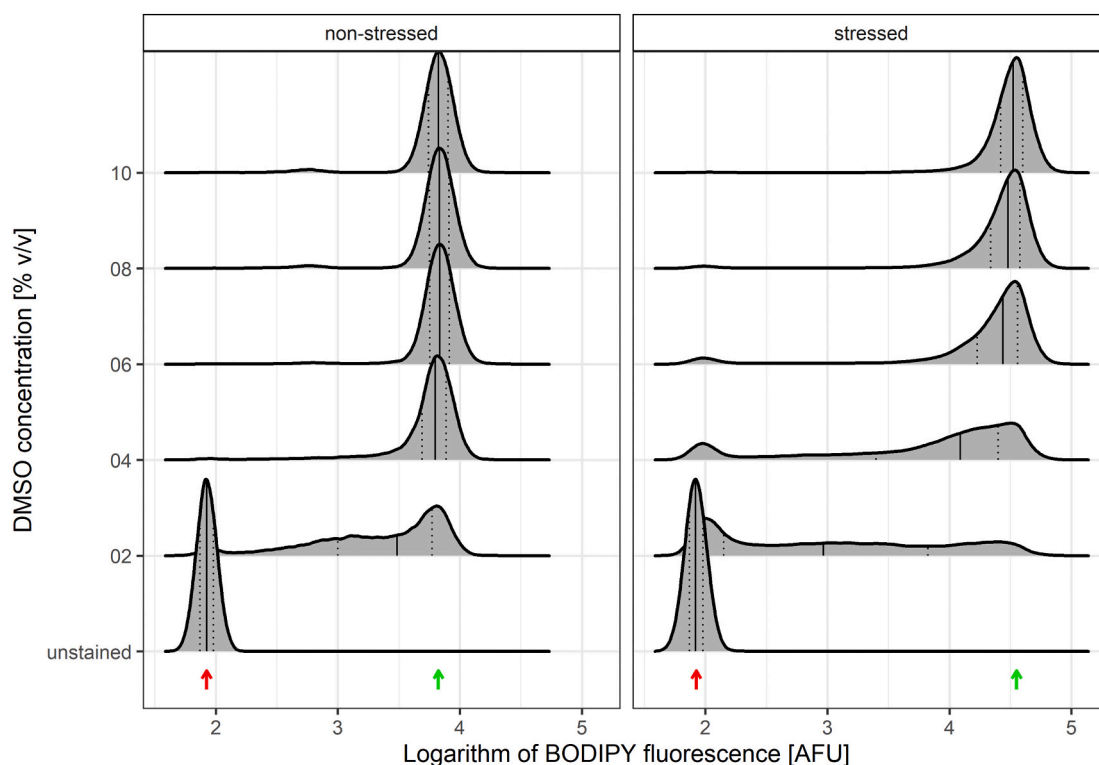


Fig. 1. Representative density curves for single cell BODIPY fluorescence emission in samples treated with different DMSO concentrations. Nutrient-replete (non-stressed) and N-deprived (stressed) *N. oceanica* cultures were treated with 5 different DMSO concentrations and $0.8 \mu\text{g ml}^{-1}$ BODIPY for 15 min and subjected to flow cytometry analysis. The density curves represent the frequency distribution of events in the green fluorescence channel, capturing cellular BODIPY fluorescence emission. The red and green arrows mark the position of peaks corresponding to non-stained and fully stained cells respectively. Solid vertical lines indicate the median of the distribution and dotted lines denote the border between the first and second and between the third and fourth quartile. With higher DMSO concentrations the fraction of unstained and intermediately stained cells decreases and the average BODIPY signal increases up to the optimal values of 6 and 10% DMSO for non-stressed and stressed cultures respectively. Samples treated with 0–10% DMSO and no BODIPY showed identical fluorescence distributions, exemplarily represented as ‘unstained’. (For interpretation of the references to colour in this figure legend, the reader is referred to the web version of this article.)

2.3. Staining of *N. oceanica* with BODIPY

Fresh *N. oceanica* cultures were diluted to $\sim 4 \times 10^6$ cells ml^{-1} with ASW and kept at 22°C prior to any treatment. BODIPY 505/515 (Invitrogen #D3921, hereafter referred to as BODIPY) was dissolved in DMSO at 4 mg ml^{-1} and diluted with DMSO to different working stock concentrations. Cell suspensions were supplemented with the appropriate BODIPY working stock to a specific DMSO concentration between 2 and 10% (v/v) with final BODIPY concentrations between 0.8 and $4 \mu\text{g ml}^{-1}$. Pure DMSO was used for control treatments. Upon addition of the dye, samples were vortexed for 5 s and then incubated in the dark for 15 min before flow cytometric analysis, if not indicated otherwise. For all experiments with unstressed cells, microalgal cultures were harvested during the mid-exponential stage at an OD_{750} of 0.6–0.8. For stressing cells, microalgal cultures were harvested during the mid-exponential stage at an OD_{750} of 0.6–0.8, washed twice with ASW–N, resuspended in ASW–NB–N to an OD_{750} of 0.2 and cultivated for 3 d under the previously described conditions. For experiments described under 3.5, which were conducted using the ideal staining conditions, cultures were grown under the conditions described above. On the day of analysis, 1 ml of fresh culture was diluted to $\sim 4 \times 10^6$ cells ml^{-1} with ASW and stained with 6% DMSO and $1.2 \mu\text{g ml}^{-1}$ BODIPY for 15 min (non-stressed cultures) or with 10% DMSO and $1.6 \mu\text{g ml}^{-1}$ BODIPY for 36 min (stressed cultures) before flow cytometry analysis. The rest of the culture was immediately used for quantification of neutral lipids via GC–FID (Section 2.6).

2.4. Viability assessment

Treated samples were sorted onto single-well agar plates using the cell sorter SH800S in a 384-well layout. The cell sorter was operated with a $100 \mu\text{m}$ nozzle chip and operational settings of a sample pressure of 1 and sorting mode “single cells 3 droplets”, specified in the SH800S software. 96 single cells were randomly selected from the cell population with a typical chlorophyll autofluorescence signal (Fig. S1G) and sorted per treatment in quadruplicate. Agar plates were incubated for 4 weeks before surviving colonies were counted.

2.5. Evaluation of staining duration

Real-time flow cytometry analysis was conducted by immediately subjecting a microalgal suspension to flow cytometry analysis after addition of the BODIPY/DMSO staining stock and 5 s of mixing. The data over time was binned into 24 s intervals and the median of the green fluorescence signal of all noise-corrected events was extracted per bin. Median fluorescence values of only DMSO-treated controls were subtracted from median fluorescence values of the samples and these corrected median values were normalized to their maximum value. The relative corrected median fluorescence was averaged for 3 replicate runs and analyzed as $\text{mean} \pm \text{standard deviation}$.

2.6. Quantification of neutral lipids via gas chromatography

Cellular neutral lipid contents were determined using a modified version of the protocol described by Remmers et al. [52]. Briefly, microalgal cultures were harvested by centrifugation ($4000 \times g$, 10 min)

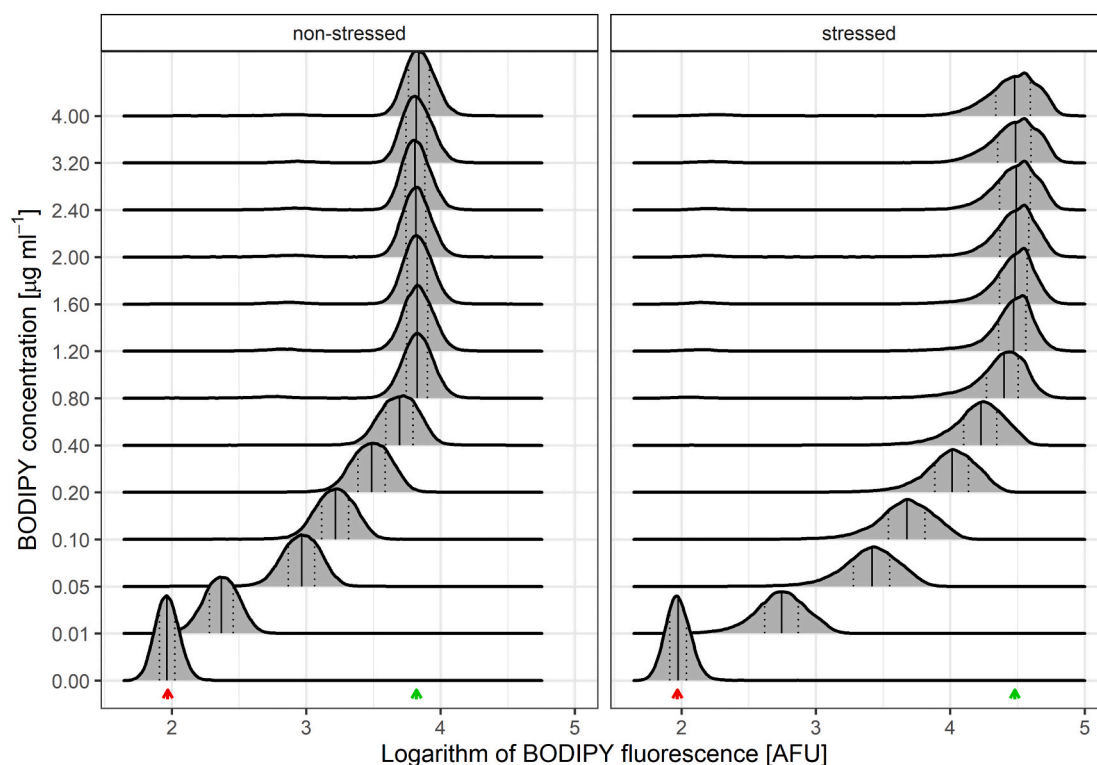


Fig. 2. Representative density curves for single cell BODIPY fluorescence emission in samples treated with different BODIPY concentrations. Nutrient-replete (non-stressed) and N-deprived (stressed) *N. oceanica* cultures were treated with 10% DMSO and 12 different BODIPY concentrations for 15 min and analyzed by flow cytometry. The density curves represent the frequency distribution of events in the green fluorescence channel. The red and green arrows mark the position of peaks corresponding to non-stained and fully stained cells respectively. Solid vertical lines indicate the median of the fluorescence distribution and dotted lines denote the border between the first and second as well as between the third and fourth quartile. $0.8 \mu\text{g ml}^{-1}$ BODIPY is sufficient to stain non-stressed wild type *N. oceanica* cells, whereas $1.2 \mu\text{g ml}^{-1}$ is required for stressed cultures. This difference is possibly related to higher intracellular TAG contents of microalgal cells under stress conditions. Higher concentrations than $2.0 \mu\text{g ml}^{-1}$ BODIPY resulted in an increased kurtosis of fluorescence distributions of stressed cells. (For interpretation of the references to colour in this figure legend, the reader is referred to the web version of this article.)

and resuspended in 1 ml of ASW. Cell concentration was determined using a Beckman Coulter Multisizer 3 (Beckman Coulter Inc., USA, 50 μm orifice) and 300 μl of the suspension was subjected to fatty acid extraction, separation into TAG and polar acyl lipids and quantification according to Remmers et al. [52]. The biomass was freeze-dried, subjected to mechanical cell disruption and lipid extraction with a chloroform:methanol (1:1.25) solution containing the 2 internal standards tripentadecanoic (T4257; Sigma-Aldrich) and 1,2-didecanoil-*sn*-glycero-3-phospho-(1'-*rac*-glycerol) (840434, Avanti Polar Lipids Inc.) at 78 $\mu\text{g ml}^{-1}$ and 75 $\mu\text{g ml}^{-1}$ respectively. Polar and apolar lipids were separated using Sep-Pak Vac silica cartridges (6 cm^3 , 1000 mg; Waters). Neutral lipids were eluted with a hexane:diethylether (7:1 v/v) solution, methylated in 5% (v/v) H_2SO_4 -containing MeOH, extracted with hexane and subjected to gas chromatography with flame-ionization detection (GC-FID). Total fatty acids were quantified based on the relative responses of individual fatty acids compared to the signal of the internal standard and normalized to the cell concentration.

2.7. Statistical data treatment

Association of two variables was tested using Pearson's product-moment correlation, indicated as r [53]. First, data were tested for univariate normality of underlying distributions using Shapiro-Wilk's test for normality [54] and for heteroscedasticity using the Breusch-Pagan test [55]. If univariate normality or homoscedasticity could not be assumed, monotonic relationship between variables was tested using Spearman's rank correlation, indicated as r_s [56]. Data presented in Section 3.4 were specifically tested for negative association between viability as a dependent variable and chemical concentrations as

independent variables. Differences between the means of two normally-distributed groups were tested using independent two-sample t -tests. α was set to 0.05 for all statistical tests. All statistical data analysis was carried out using R statistical computing software [47].

3. Results and discussion

3.1. The dimethyl sulfoxide concentration required to permeabilize *N. oceanica* cells depends on cellular physiology

It was previously demonstrated that DMSO is required to facilitate BODIPY uptake in *Nannochloropsis* by Brennan and co-workers [29]. The authors reported that concentrations lower than 6% (v/v) caused incomplete staining in a subpopulation of cells. Although treatment with 6% DMSO resulted in a homogeneous signal and was selected as the optimal DMSO concentration for non-stressed *N. oculata* in their study, the applicability of the protocol for stressed cells remained unclear. However, screening of microalgae for elevated lipid contents is promising especially when using stressed cultures that are overproducing lipids [36]. In order to develop a universally applicable *N. oceanica* lipid staining protocol that can be used in high-throughput screening studies, we investigated the effect of varying DMSO and BODIPY concentrations on fluorescence signal intensity in both, stressed and non-stressed cells.

First, we elucidated the effect of different solvent concentrations on the permeabilization of microalgal cells. A non-stressed, exponentially growing culture of *N. oceanica* and one that was stressed by cultivation in N-depleted media for 3 d were subjected to BODIPY staining using 2–10% (v/v) DMSO at a fixed BODIPY concentration of $0.8 \mu\text{g ml}^{-1}$ for 15 min. Single cell fluorescence was quantified using flow cytometry

analysis, statistical software and an automated gating pipeline (supplementary Fig. S1) for removal of noise. Fig. 1 shows the distribution of single cell fluorescence in the green channel, capturing the emission of BODIPY. Unstained controls were treated with 0–10% DMSO but no BODIPY, and displayed the same signal distribution regardless of solvent concentration. This signal (“unstained” in Fig. 1) represents the autofluorescence of cells in the green spectrum. Homogeneously stained samples were expected to produce unimodal Poisson distributions on a log-scale, as is common for flow cytometry data [57]. Bimodal distributions or multiple peaks indicated heterogeneously stained samples with a subpopulation of cells that was either unstained or only partially stained. The positions of peaks corresponding to unstained and fully stained cells are highlighted by red and green arrows respectively.

Non-stressed cells appear to be effectively permeabilized by treatment with DMSO concentrations of 6% or higher because no difference can be seen for fluorescence distributions of samples treated with 6–10% DMSO, indicated by identical median values (solid vertical lines in Fig. 1) and interquartile ranges (IQRs, dotted vertical lines in Fig. 1) of the distributions. Samples treated with 2% DMSO showed a substantial fraction of unstained and partially stained cells and treatment with 4% DMSO resulted in negative skewness of the distribution compared to samples treated with 6–10% DMSO. Stressed cells require treatment with 10% DMSO, as samples that were treated with 8% or lower show a fraction of completely unstained cells (lefthand peak) and a lower fluorescence signal of stained cells. Based on these results we concluded that (i) stressed cells require higher concentrations of solvent for cell permeabilization and (ii) 10% DMSO facilitate complete dye uptake in *N. oceanica* regardless of physiological state.

Our findings regarding a subpopulation of *N. oceanica* cells being insufficiently permeabilized when treated with less than 6% DMSO are in good agreement with observations made by Brennan et al. [29] for non-stressed *Nannochloropsis oculata*. We were able to establish that this phenomenon is even more pronounced for stressed compared to non-stressed cells but it remains unclear which factors contribute to culture heterogeneity with regard to permeabilization. During flow cytometry analysis of samples that had been treated with suboptimal DMSO concentrations, partially and fully stained cell populations showed identical forward scatter distributions (data not shown). Because forward scatter is a proxy for particle size, we can conclude that cell size is not a relevant parameter for permeabilization. When applying DMSO concentrations >6%, we did not find a decrease in BODIPY fluorescence signal. This is in contrast to what was observed for BODIPY staining of *N. oculata* [29] and other microalgal genera. For instance, Cirulis et al. [58] found an inhibitory effect of DMSO at concentrations >1% (v/v) on BODIPY fluorescence intensity when staining *Scenedesmus* and *Chlorella*, concomitant with a substantial decrease in intact cells and an increase in cell debris. The drastically different response of *Scenedesmus* and *Chlorella* to elevated DMSO concentrations compared to what we report for *N. oceanica* highlights the need for attentiveness when adapting laboratory protocols for use with other species. An obvious reason for this is the high evolutionary diversity of the polyphyletic group of microalgae which implicates a highly variable cell morphology and physiology among different genera.

Insufficient dye penetration using conventional staining protocols has previously been reported for several stains with different *Nannochloropsis* species [29,32,33,35] and it is usually attributed to the comparably thick, scaly cell wall of this genus. It is, therefore, reasonable to assume that the increased solvent concentrations necessary to stain stressed *N. oceanica* cells in our study are related to a change in the cell wall ultrastructure compared to non-stressed cells. This hypothesis is in good agreement with results of previous studies, which showed that cell wall thickness of *Nannochloropsis* increases up to >50% under N-deprivation and other stress conditions [46,59,60]. Whereas the interaction between DMSO and lipid membranes is well-studied [61–63], an interaction model for the solvent with cell walls of living organisms has never been reported. However, experimental evidence exists for the

ability of DMSO to disrupt intra- and intermolecular H-bonds in cellulose and other plant cell wall polysaccharides, as it is capable of solubilizing these compounds in vitro when applied together with LiCl [64–66]. Thus, an interaction of DMSO with the primary *Nannochloropsis* cell wall constituent cellulose [46,67] is a potential explanation for our observation that higher solvent concentrations facilitate cell permeation under conditions of increased cell wall thickness, which warrants further investigation.

3.2. The minimum BODIPY concentration necessary for full staining depends on cellular triacylglyceride contents

In consequence of the previous results, 10% DMSO was chosen as a fixed solvent concentration for investigating the effect of BODIPY concentration on fluorescence intensity. We treated non-stressed and stressed cultures with 12 different BODIPY concentrations, namely 0.01, 0.05, 0.1, 0.2, 0.4, 0.8, 1.2, 1.6, 2.0, 2.4, 3.2 and 4.0 $\mu\text{g ml}^{-1}$ for 15 min. The experiment revealed that 0.8 $\mu\text{g ml}^{-1}$ BODIPY is sufficient to completely stain exponentially growing *N. oceanica* and that higher BODIPY concentrations have no effect on the fluorescence distribution (Fig. 2). Stressed cells however required treatment with 1.2 $\mu\text{g ml}^{-1}$ BODIPY, as treatment with 0.8 $\mu\text{g ml}^{-1}$ resulted in a lower median fluorescence signal. This was also seen when conducting the experiment with DMSO concentrations other than 10% (supplementary Fig. S2). Presumably, the increased TAG contents of cells grown under stress conditions compared to that of non-stressed cells necessitates higher concentrations of dye to achieve full staining of lipid bodies. Considering this possible link between cellular TAG content and required dye concentration, an ideal staining protocol should feature BODIPY concentrations of 1.6 $\mu\text{g ml}^{-1}$ to be suitable for identifying strains with higher lipid contents than the wild type strain investigated here. Under this premise, 1.2 $\mu\text{g ml}^{-1}$ BODIPY would likely be sufficient for screening of non-stressed microalgal cultures as the wild type is completely stained with 0.8 $\mu\text{g ml}^{-1}$ under these conditions (Fig. 2). BODIPY concentrations higher than 2.0 $\mu\text{g ml}^{-1}$ are not advisable because they resulted in an increased kurtosis and IQR of fluorescence distributions in our experiments with stressed cells (Fig. 2), possibly due to formation of staining artifacts.

3.3. Optimal staining duration depends on cellular physiology

In the study of fluorophores an optimization of the staining duration is important for several reasons. First, several fluorogenic molecules such as Nile Red are prone to photobleaching, a process of photochemical alterations when in a radiation-induced state of excitation which causes the dye to degrade over time [28,68]. When incubated in the dark, non-radiation-induced dye inactivation presumably through interaction with reactive oxygen species can further result in a decrease in active dye molecules [69–72], which was, i.a., shown for Nile Red inactivation inside microalgal cells [73]. Second, dye uptake is highly dependent on chemical properties of the fluorophore and on cell physiology, especially on the structure of the cell barrier. Incomplete staining of target compounds in consequence of an insufficient staining duration can cause a strongly shifting signal over time, high variability between samples and an underestimation of target molecules. Third, when staining is combined with the isolation of viable cells, exposure to dye and solvent need to be minimized to forestall unnecessary toxic effects. Furthermore, excessive staining duration can lead to metabolic changes in non-fixed cells or it can cause cellular decomposition in the presence of solvents.

In literature dealing with BODIPY staining of *Nannochloropsis* typical incubation durations range between 5 and 30 min [27,29,74–76] without discrimination between different physiological states of microalgal cells. Real-time flow cytometric analysis has proven as a powerful approach for measuring molecular interactions and cellular responses to external stimuli [77–79] so we deployed this technique to monitor the dye uptake in *N. oceanica*. Cells from a stressed and non-

stressed culture were stained with $1.2 \mu\text{g ml}^{-1}$ BODIPY and 10% or 6% DMSO respectively, as these concentrations were found to induce the highest signal intensities in our previous experiments. Fig. 3 illustrates the development of the background-corrected, median BODIPY fluorescence intensity relative to its maximum signal over time. The maximum fluorescence intensity was reached around 15 min for non-stressed cells, whereas stressed cells displayed a stable signal after ~ 36 min, although 90% of the maximum intensity was reached after 22 min with only gradual signal increases after that point. For both culture states the initial increases in fluorescence intensity were low and linear with a surge around 3 min of staining. After this, the fluorescence signal development was well described by an adjusted Michaelis-Menten model (data not shown).

In light of these findings, the experiment described under Section 3.2 was performed with stressed cultures using a staining duration of 36 min (Fig. S3). No substantial differences were seen regarding the optimal dye concentration compared to results obtained when staining for 15 min, although kurtosis increase for BODIPY concentrations greater than $2 \mu\text{g ml}^{-1}$ was less pronounced with 36 min staining.

3.4. The impact of staining and sorting on cell viability depends on the BODIPY concentration

Optimizing the impact of BODIPY treatment on cell viability is crucial in order to develop a protocol that is suitable for coupling in vivo lipid staining to cell sorting. Proper experimental design of high-throughput screenings requires knowledge of the fraction of cells that can be expected to survive the procedure. Because in high-throughput screenings cells are exposed to chemical stress during the staining and to physical stress during sorting, we designed an experiment that factors in both stressors. Non-stressed and stressed cultures were treated with 0–10% DMSO (Fig. 4A) and 0–4 $\mu\text{g ml}^{-1}$ BODIPY (Fig. 4C) for 15 and 36 min respectively and single cells were sorted onto agar plates using a

fluorescence-activated cell sorter. The fraction of viable cells was determined as the percentage of single cells that were able to grow into colonies within 4 weeks (Fig. 4).

We found that cultures in different growth stages have a profoundly different tolerance toward stress inflicted by staining and sorting. When no BODIPY was applied during treatment, no significant negative correlation between DMSO concentration and cell viability was observed (Fig. 4A, Pearson correlation coefficients $r(22) = 0.39$, $p = 0.972$ and $r(22) = 0.23$, $p = 0.865$ for non-stressed and stressed cultures respectively). Therefore, all data for DMSO-only treated samples were pooled and tested for differences in post-sort viability between non-stressed and stressed cultures (Fig. 4B). We found that non-stressed cells ($M = 91$, $SD = 3.5$) recovered slightly better after cell sorting compared to stressed cells ($M = 87.8$, $SD = 2.1$), $t(43) = 6.3$, $p < 0.001$, which can be attributed to an increased susceptibility of stressed cells to adverse effects of staining and cell sorting or to lower pre-sort viabilities. When treatment was conducted with 10% DMSO and different BODIPY concentrations (Fig. 4C), no significant effect of staining treatment on viability was found for unstressed cells (Spearman's ρ $r_s = 0.07$, $p = 0.655$). For stressed cultures however, BODIPY concentration was negatively correlated with cell viability ($r_s = -0.34$, $p = 0.027$). Because we observed no significant fluorescence increase for BODIPY concentrations greater than $1.2 \mu\text{g ml}^{-1}$ (Fig. 2), this concentration is likely preferable when high cell viabilities are required.

The average post-sort reproductive viability that we observed for unstressed, DMSO-only treated *N. oceanica* (91%) is high when compared to values reported for other microalgae. Pereira and co-workers found an average of 70% viability when sorting microalgal communities [80], which is already more than the 20–30% viability reported by Sensen et al. [81]. Because shear forces are the most common stressor during FACS [82], the strong resilience of *N. oceanica* cells to sorting is likely related to good cellular properties for high shear resistance. Several features of *Nannochloropsis* cell physiology such as a small cell size, the absence of flagella, and presence of a rigid, cellulose containing cell wall [67] have been proposed to be associated with high shear resistance [83], supporting this notion. In this regard, it may seem contradictory that stressed *N. oceanica* cells show an increase in cell wall thickness but a decrease in post-sort viability compared to non-stressed cells. However, previous studies have indicated that cell wall thickness is not necessarily correlated with tensile and shear resistance of microalgal cells [46,83,84].

3.5. The staining procedure allows for accurate prediction of lipid contents

After deciphering the optimal conditions for staining cells that were incubated under different nutrient regimes we wanted to validate our improved staining procedure by determining how accurately it translates to cellular neutral lipid contents. We applied the procedure to 18 independent *N. oceanica* cultures, quantified the fluorescence emission and compared the results to cellular neutral lipid contents determined by a reference procedure involving gas chromatography and cell counting [52]. Fig. 5 shows the median of the background-corrected single cell BODIPY fluorescence levels plotted against the content of neutral lipids per cell. To cover a broad range of lipid contents in a single experiment, half of the microalgal cultures were harvested during the mid-exponential growth phase, the other half was starved of N for 72 h prior to analysis. We found an excellent correlation between fluorescence intensities of *N. oceanica* cells stained with the optimized protocol (6% DMSO and $1.2 \mu\text{g ml}^{-1}$ BODIPY for 15 min for replete cultures, 10% DMSO and $1.6 \mu\text{g ml}^{-1}$ BODIPY for 36 min for deplete cultures) and cellular neutral lipid contents, with a coefficient of determination of $R^2 = 0.981$. Evidently, the optimized procedure has high predictive power for cellular neutral lipid contents in *N. oceanica*. When regression analysis was carried out based on data from cultures within the same growth stage only (Fig. 5, dotted gray lines), the coefficient of determination

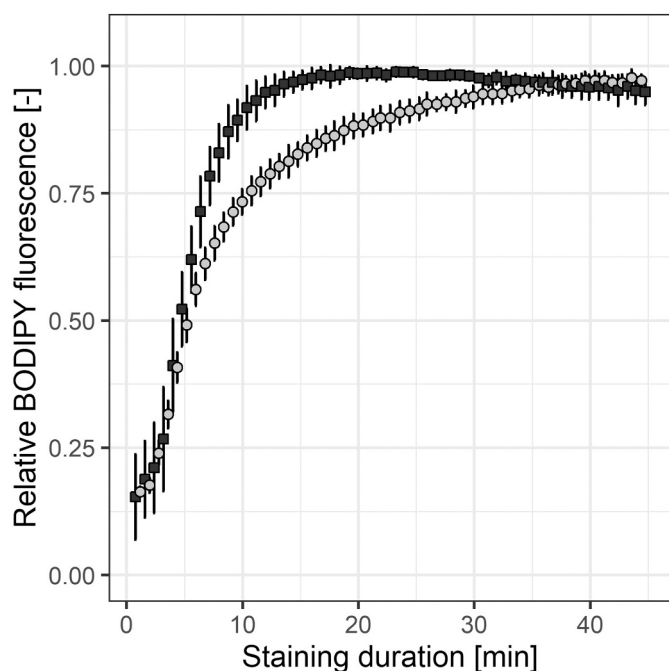


Fig. 3. Effect of staining duration on single cell fluorescence emission for unstressed (■) and stressed (○) *N. oceanica* cultures. With optimal BODIPY and DMSO concentrations, unstressed microalgal cells are stained rapidly and achieve full staining within 15 min. Stressed cultures achieve full staining after ~ 36 min. Fluorescence values shown are the mean \pm SD of the median of the fluorescence distribution observed in $n = 3$ algae cultures relative to its maximum value per sample.

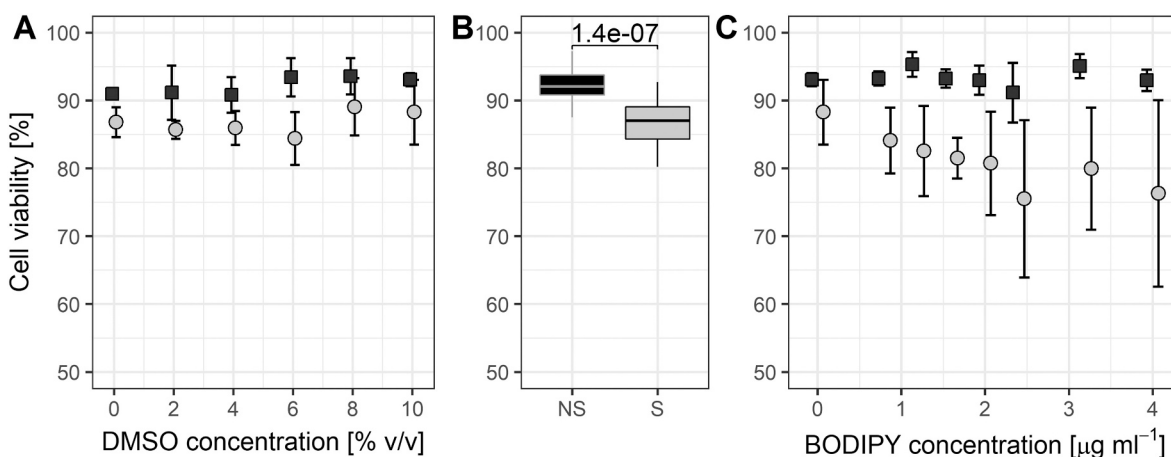


Fig. 4. Impact of staining and sorting on cell viability of non-stressed (■) and stressed (○) *N. oceanica* cells. (A) Cultures were treated with DMSO only and subjected to cell sorting. Viabilities are given as the mean \pm SD of $n = 4$ replicate cultures. The results show that exposure to the solvent alone without application of BODIPY does not impair cell viability regardless of culture state. (B) For DMSO-only treatments, stressed (S) cultures showed an overall decrease in cell viability compared to non-stressed (NS) cultures, which can be attributed to an increased sensitivity toward sorting stress or to a lower pre-sort viability. (C) Cultures were treated with 10% DMSO and varying BODIPY concentrations before being subjected to cell sorting. Non-stressed cells were not affected by staining and survival rates showed no significant correlation with BODIPY concentration whereas stressed cells showed a decline in viability with higher BODIPY concentrations.

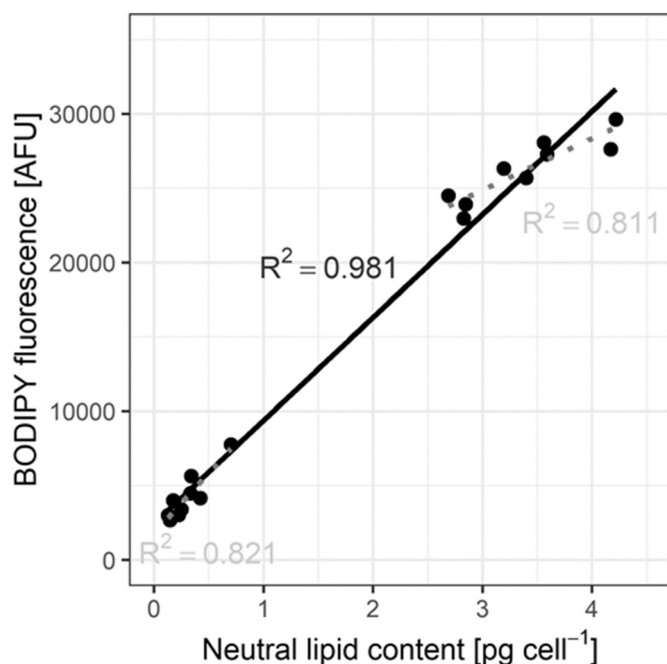


Fig. 5. Correlation between BODIPY fluorescence and cellular neutral lipid content. With the optimized staining procedure we found a highly significant linear correlation between cellular neutral lipid content and median BODIPY fluorescence. The R^2 value (0.981) of this correlation greatly exceeds previously reported values and suggests that the optimized protocol allows for an absolute quantification of cellular neutral lipids in the range of 0.1–4 pg cell⁻¹, which roughly corresponds to 3–45% of neutral lipids per dry biomass for *N. oceanica*.

remained high ($R^2 > 0.8$). This suggests that the optimized procedure will allow to distinguish between strains with similar neutral lipid contents.

Several correlation curves have been established for staining of microalgae with Nile Red, some of which had R^2 values of 0.95 or higher, for example for species belonging to the genera *Botryococcus* [85], *Isochrysis* [86], *Chlorella* [87], and *Scenedesmus* [58]. Far fewer reports exist for correlations between probe fluorescence and lipid content when using BODIPY as lipophilic dye [58,88] and none of them

for *Nannochloropsis*, despite major advantages of BODIPY compared to Nile Red, including high specificity for neutral lipids, stronger signal and better photostability [29,89]. Whereas qualitative or semi-quantitative lipid estimations can suffice for some high-throughput screening procedures, our improved staining protocol will facilitate a sophisticated screening with high accuracy in neutral lipid quantification and minimum impact on cell viability. Moreover, the good translatability of fluorescence values to cellular neutral lipids suggests that our staining protocol could replace cumbersome and expensive lipid quantification procedures, which typically rely on solvent-based extraction coupled to gravimetric or GC analysis.

4. Conclusion

We have developed a robust and simple staining protocol for *N. oceanica* with good translatability of fluorescence values to neutral lipid contents. We found that cellular physiology strongly affects the staining conditions necessary for complete cell barrier permeabilization and dye uptake. Exponentially growing cells are readily stained with a treatment of 6% DMSO and 1.2 $\mu\text{g ml}^{-1}$ BODIPY for 15 min whereas N-stressed cultures require 10% DMSO and 1.2–1.6 $\mu\text{g ml}^{-1}$ BODIPY for 36 min for complete staining. When coupling these lipid staining protocols to cell sorting, viabilities of ~91% and 83–82% can be expected for unstressed and stressed cells respectively. The optimized screening procedure will no doubt aid in the identification of *N. oceanica* strains with elevated neutral lipid contents in future studies.

CRediT author contribution statement

CS: Conceptualization, Methodology, Investigation, Validation, Software, Formal analysis, Writing - original draft, Writing - review & editing. **MH:** Conceptualization, Methodology, Investigation. **SD:** Conceptualization, Project administration, Supervision, Writing - review & editing. **RHW:** Project administration, Supervision, Writing - review & editing, Funding acquisition. **MJB:** Project administration, Supervision, Writing - review & editing.

Statement of informed consent, human/animal rights

No conflicts, informed consent, or human or animal rights are applicable to this study.

Declaration of competing interest

The authors declare that they have no known competing financial interests or personal relationships that could have appeared to influence the work reported in this paper.

Acknowledgements

This work was funded by the Netherlands Organisation for Scientific Research (NWO) Buildings Blocks of Life programme (grant number 737.016.007).

Appendix A. Supplementary data

Supplementary data to this article can be found online at <https://doi.org/10.1016/j.algal.2020.102138>.

References

- [1] X. Deng, Y. Li, X. Fei, Microalgae: a promising feedstock for biodiesel, *Afr. J. Microbiol. Res.* 3 (2009) 1008–1014, <http://www.biodiesel.org>.
- [2] R.H. Wijffels, M.J. Barbosa, An Outlook on Microalgal Biofuels 329, 2010, pp. 796–799, <https://doi.org/10.1126/science.1189003>.
- [3] H. Goold, F. Beisson, G. Peltier, Y. Li-Beisson, Microalgal Lipid Droplets: Composition, Diversity, Biogenesis and Functions 34, 2015, pp. 545–555, <https://doi.org/10.1007/s00299-014-1711-7>.
- [4] M.A. Islam, M. Magnusson, R.J. Brown, G.A. Ayoko, M.N. Nabi, K. Heimann, Microalgal species selection for biodiesel production based on fuel properties derived from fatty acid profiles, *Energies*. 6 (2013) 5676–5702, <https://doi.org/10.3390/en6115676>.
- [5] X.N. Ma, T.P. Chen, B. Yang, J. Liu, F. Chen, Lipid production from *Nannochloropsis*, *Mar. Drugs* 14 (2016) 61, <https://doi.org/10.3390/md14040061>.
- [6] J. Liu, Y. Song, W. Qiu, Oleaginous microalgae *Nannochloropsis* as a new model for biofuel production: review & analysis, *Renew. Sust. Energ. Rev.* 72 (2017) 154–162, <https://doi.org/10.1016/j.rser.2016.12.120>.
- [7] G. Chini Zittelli, F. Lavista, A. Bastianini, L. Rodolfi, M. Vincenzini, M.R. Tredici, Production of eicosapentaenoic acid by *Nannochloropsis* sp. cultures in outdoor tubular photobioreactors, *J. Biotechnol.* (1999) 299–312, [https://doi.org/10.1016/S0168-1656\(99\)00082-6](https://doi.org/10.1016/S0168-1656(99)00082-6) (Elsevier Sci B.V.).
- [8] S. Archambault, C.M. Starbuck Downes, W. Van Voorhies, C.A. Erickson, P. Lammers, *Nannochloropsis* sp. algae for use as biofuel: analyzing a translog production function using data from multiple sites in the southwestern United States, *Algal Res.* 6 (2014) 124–131, <https://doi.org/10.1016/j.algal.2014.10.005>.
- [9] A. San Pedro, C.V. González-López, F.G. Ación, E. Molina-Grima, Outdoor pilot production of *nannochloropsis gaditana*: influence of culture parameters and lipid production rates in raceway ponds, *Algal Res.* 8 (2015) 205–213, <https://doi.org/10.1016/j.algal.2015.02.013>.
- [10] Y. Ma, Z. Wang, C. Yu, Y. Yin, G. Zhou, Evaluation of the potential of 9 *Nannochloropsis* strains for biodiesel production, *Bioresour. Technol.* 167 (2014) 503–509, <https://doi.org/10.1016/j.biortech.2014.06.047>.
- [11] J. Ruiz, G. Olivieri, J. De Vree, R. Bosma, P. Willems, J.H. Reith, M.H.M. Eppink, D. M.M. Kleinegris, R.H. Wijffels, M.J. Barbosa, Towards Industrial Products From Microalgae 9, 2016, pp. 3036–3043, <https://doi.org/10.1039/c6ee01493c>.
- [12] P. Hyka, S. Lickova, P. Pribyl, K. Melzoch, K. Kovar, Flow Cytometry for the Development of Biotechnological Processes With Microalgae 31, 2013, pp. 2–16, <https://doi.org/10.1016/j.biotechadv.2012.04.007>.
- [13] H. Pereira, P.S.C. Schulze, L.M. Schüler, T. Santos, L. Barreira, J. Varela, Fluorescence Activated Cell-sorting Principles and Applications in Microalgal Biotechnology 30, 2018, pp. 113–120, <https://doi.org/10.1016/j.algal.2017.12.013>.
- [14] E.A. Specht, E. Braselmann, A.E. Palmer, A critical and comparative review of fluorescent tools for live-cell imaging, *Annu. Rev. Physiol.* 79 (2017) 93–117, <https://doi.org/10.1146/annurev-physiol-022516-034055>.
- [15] P. Greenspan, E.P. Mayer, S.D. Fowler, Nile red: a selective fluorescent stain for intracellular lipid droplets, *J. Cell Biol.* 100 (1985) 965–973, <https://doi.org/10.1083/jcb.100.3.965>.
- [16] V. Martinez, M. Henary, Nile Red and Nile Blue: Applications and Syntheses of Structural Analogues 22, 2016, pp. 13764–13782, <https://doi.org/10.1002/chem.201601570>.
- [17] C.A. Guido, B. Mennucci, D. Jacquemin, C. Adamo, Planar vs. twisted intramolecular charge transfer mechanism in Nile Red: new hints from theory, *Phys. Chem. Chem. Phys.* 12 (2010) 8016–8023, <https://doi.org/10.1039/b927489h>.
- [18] T.K. Fam, A.S. Klymchenko, M. Collot, Recent Advances in Fluorescent Probes for Lipid Droplets 11, 2018, <https://doi.org/10.3390/ma11091768>.
- [19] J. Koreiviënė, Microalgal lipid staining with Fluorescent BODIPY dye, in: *Methods in Molecular Biology*, Humana Press Inc., 2020, pp. 47–53, <https://doi.org/10.1007/97810712017101>.
- [20] M. Collot, T.K. Fam, P. Ashokkumar, O. Faklaris, T. Galli, L. Danglot, A. S. Klymchenko, Ultrabright and fluorogenic probes for multicolor imaging and tracking of lipid droplets in cells and tissues, *J. Am. Chem. Soc.* 140 (2018) 5401–5411, <https://doi.org/10.1021/jacs.7b12817>.
- [21] H.J. Yang, C.L. Hsu, J.Y. Yang, W.Y. Yang, Monodansylpentane as a blue-fluorescent lipid-droplet marker for multi-color live-cell imaging, *PLoS One* 7 (2012), e32693, <https://doi.org/10.1371/journal.pone.0032693>.
- [22] S.K. Gidda, S. Park, M. Pyc, O. Yurchenko, Y. Cai, P. Wu, D.W. Andrews, K. D. Chapman, J.M. Dyer, R.T. Mullen, Lipid droplet-associated proteins (LDAPs) are required for the dynamic regulation of neutral lipid compartmentation in plant cells, *Plant Physiol.* 170 (2016) 2052–2071, <https://doi.org/10.1104/pp.15.01977>.
- [23] S. Kuntam, L.G. Puskás, F. Ayaydin, Characterization of a new class of blue-fluorescent lipid droplet markers for live-cell imaging in plants, *Plant Cell Rep.* 34 (2015) 655–665, <https://doi.org/10.1007/s00299-015-1738-4>.
- [24] S. Harchouni, B. Field, B. Menand, AC-202, a highly effective fluorophore for the visualization of lipid droplets in green algae and diatoms, *Biotechnol. Biofuels* 11 (2018) 120, <https://doi.org/10.1186/s13068-018-1117-9>.
- [25] S.I. Suarez, C.C. Warner, H. Brown-Harding, A. Thooft, B. VanVeller, J. Lukesh, Selective staining and quantification of intracellular lipid droplets with CBD-fluor, a new and versatile push-pull fluorophore, *ChemRxiv* (2019), <https://doi.org/10.26434/chemrxiv.8872634.v1> (doi:10.26434/CHEMRXIV.8872634.V1).
- [26] S.I. Suarez, C.C. Warner, H. Brown-Harding, A.M. Thooft, B. VanVeller, J.C. Lukesh, Highly selective staining and quantification of intracellular lipid droplets with a compact push-pull fluorophore based on benzothiadiazole, *Org. Biomol. Chem.* 18 (2020) 495–499, <https://doi.org/10.1039/c9ob02486g>.
- [27] T. Govender, L. Ramanna, I. Rawat, F. Bux, BODIPY staining, an alternative to the Nile Red fluorescence method for the evaluation of intracellular lipids in microalgae, *Bioresour. Technol.* 114 (2012) 507–511, <https://doi.org/10.1016/j.biortech.2012.03.024>.
- [28] J. Rumin, H. Bonnefond, B. Saint-Jean, C. Rouxel, A. Sciadra, O. Bernard, J. P. Cadoret, G. Bougaran, The use of fluorescent Nile red and BODIPY for lipid measurement in microalgae, *Biotechnol. Biofuels* 8 (2015) 42, <https://doi.org/10.1186/s13068-015-0220-4>.
- [29] L. Brennan, A. Blanco Fernández, A.S. Mostaert, P. Owende, Enhancement of BODIPY 505/515 lipid fluorescence method for applications in biofuel-directed microalgal production, *J. Microbiol. Methods* 90 (2012) 137–143, <https://doi.org/10.1016/j.mimet.2012.03.020>.
- [30] T.A. Beacham, V.M. Macia, P. Rooks, D.A. White, S.T. Ali, Altered lipid accumulation in *Nannochloropsis salina* CCAP849/3 following EMS and UV induced mutagenesis, *Biotechnol. Rep.* 7 (2015) 87–94, <https://doi.org/10.1016/j.btre.2015.05.007>.
- [31] H. Osorio, C. Jara, K. Fuenzalida, E. Rey-Jurado, M. Vásquez, High-efficiency nuclear transformation of the microalga *Nannochloropsis oceanica* using Tn5 Transposome for the generation of altered lipid accumulation phenotypes, *Biotechnol. Biofuels* 12 (2019) 134, <https://doi.org/10.1186/s13068-019-1475-y>.
- [32] M.J.W. Veldhuis, T.L. Cucci, M.E. Sieracki, Cellular DNA content of marine phytoplankton using two new fluorochromes: taxonomic and ecological implications, *J. Phycol.* 33 (1997) 527–541, <https://doi.org/10.1111/j.0022-3646.1997.00527.x>.
- [33] ATLAS Collaboration, A Look Back at the U.S. Department of Energy's Aquatic Species, National Renewable Energy Laboratory (NREL), Golden, CO, 2012, <https://doi.org/10.2172/15003040>.
- [34] T.T. Yen Doan, J.P. Obbard, Enhanced lipid production in *Nannochloropsis* sp. using fluorescence-activated cell sorting, *GCB Bioenergy* 3 (2011) 264–270, <https://doi.org/10.1111/j.1757-1707.2010.01076.x>.
- [35] T.T.Y. Doan, J.P. Obbard, Improved Nile Red staining of *Nannochloropsis* sp., *J. Appl. Phycol.* 23 (2010) 895–901, <https://doi.org/10.1007/s10811-010-9608-5>.
- [36] M. Terashima, E.S. Freeman, R.E. Jinkerson, M.C. Jonikas, A fluorescence-activated cell sorting-based strategy for rapid isolation of high-lipid *Chlamydomonas* mutants, *Plant J.* 81 (2015) 147–159, <https://doi.org/10.1111/tpj.12682>.
- [37] G. Breuer, P.P. Lamers, D.E. Martens, R.B. Draaisma, R.H. Wijffels, The impact of nitrogen starvation on the dynamics of triacylglycerol accumulation in nine microalgal strains, *Bioresour. Technol.* 124 (2012) 217–226, <https://doi.org/10.1016/j.biortech.2012.08.003>.
- [38] L.D. Zhu, Z.H. Li, E. Hiltunen, Strategies for Lipid Production Improvement in Microalgae as a Biodiesel Feedstock 2016, 2016, <https://doi.org/10.1155/2016/8792548>.
- [39] G. Sibi, V. Shetty, K. Mokashi, Enhanced Lipid Productivity Approaches in Microalgae as an Alternate for Fossil Fuels – A Review 89, 2016, pp. 330–334, <https://doi.org/10.1016/j.joei.2015.03.008>.
- [40] S. Nagappan, S. Devendran, P.C. Tsai, H. Jayaraman, V. Alagarsamy, A. Pugazhendhi, V.K. Ponnusamy, Metabolomics Integrated With Transcriptomics and Proteomics: Evaluation of Systems Reaction to Nitrogen Deficiency Stress in Microalgae 91, 2020, pp. 1–14, <https://doi.org/10.1016/j.procbio.2019.11.027>.
- [41] D. Simonotto, M.A. Block, N. La Rocca, J. Jouhet, E. Maréchal, G. Finazzi, T. Morosinotto, The response of *Nannochloropsis gaditana* to nitrogen starvation includes de novo biosynthesis of triacylglycerols, a decrease of chloroplast galactolipids, and reorganization of the photosynthetic apparatus, *Eukaryot. Cell* 12 (2013) 665–676, <https://doi.org/10.1128/EC.00363-12>.
- [42] D. Han, J. Jia, J. Li, M. Sommerfeld, J. Xu, Q. Hu, Metabolic remodeling of membrane glycerolipids in the microalga *Nannochloropsis oceanica* under nitrogen deprivation, *Front. Mar. Sci.* 4 (2017) 242, <https://doi.org/10.3389/fmars.2017.00242>.

- [43] J. Li, D. Han, D. Wang, K. Ning, J. Jia, L. Wei, X. Jing, S. Huang, J. Chen, Y. Li, Q. Hu, J. Xu, Choreography of transcriptomes and lipidomes of *Nannochloropsis* reveals the mechanisms of oil synthesis in microalgae, *Plant Cell* 26 (2014) 1645–1665, <https://doi.org/10.1105/tpc.113.121418>.
- [44] H.P. Dong, E. Williams, D.Z. Wang, Z.X. Xie, R.C. Hsia, A. Jenck, R. Halden, J. Li, F. Chen, A.R. Place, Responses of *Nannochloropsis oceanica* IMET1 to long-term nitrogen starvation and recovery, *Plant Physiol.* 162 (2013) 1110–1126, <https://doi.org/10.1104/pp.113.214320>.
- [45] J. Jia, D. Han, H.G. Gerken, Y. Li, M. Sommerfeld, Q. Hu, J. Xu, Molecular mechanisms for photosynthetic carbon partitioning into storage neutral lipids in *Nannochloropsis oceanica* under nitrogen-depletion conditions, *Algal Res.* 7 (2015) 66–77, <https://doi.org/10.1016/j.algal.2014.11.005>.
- [46] S.W. Jeong, S.W. Nam, K. Hwangbo, W.J. Jeong, B.R. Jeong, Y.K. Chang, Y.I. Park, Transcriptional regulation of cellulose biosynthesis during the early phase of nitrogen deprivation in *Nannochloropsis salina*, *Sci. Rep.* 7 (2017), <https://doi.org/10.1038/s41598-017-05684-4>.
- [47] R Core Team, R: A Language and Environment for Statistical Computing, 2018 (doi:3-900051-14-3).
- [48] B. Ellis, P. Haaland, F. Hahne, N.L. Meur, N. Gopalakrishnan, flowCore: flowCore: basic structures for flow cytometry data. <http://Bioconductor.org/>, 2009.
- [49] G. Finak, flowWorkspace: a package for importing flowJo workspaces into R, in: R Guide, 2014.
- [50] V. Phu, W. Jiang, R. Gottardo, G. Finak, GgCyto: next generation open-source visualization software for cytometry, *Bioinformatics* (2018), <https://doi.org/10.1093/bioinformatics/bty441>.
- [51] R.C. Gentleman, V.J. Carey, D.M. Bates, B. Bolstad, M. Dettling, S. Dudoit, B. Ellis, L. Gautier, Y. Ge, J. Gentry, K. Hornik, T. Hothorn, W. Huber, S. Iacus, R. Irizarry, F. Leisch, C. Li, M. Maechler, A.J. Rossini, G. Sawitzki, C. Smith, G. Smyth, L. Tierney, J.Y.H. Yang, J. Zhang, Bioconductor: open software development for computational biology and bioinformatics, *Genome Biol.* 5 (2004), <https://doi.org/10.1186/gb-2004-5-10-r80>.
- [52] I.M. Remmers, A. Hidalgo-Ulloa, B.P. Brandt, W.A.C. Evers, R.H. Wijffels, P. P. Lamers, Continuous versus batch production of lipids in the microalgae *Acutodesmus obliquus*, *Bioresour. Technol.* (2017), <https://doi.org/10.1016/j.biortech.2017.04.093>.
- [53] J. Benesty, J. Chen, Y. Huang, I. Cohen, Pearson Correlation Coefficient, 2009, pp. 1–4, https://doi.org/10.1007/978-3-642-00296-0_5.
- [54] S.S. Shapiro, M.B. Wilk, An analysis of variance test for normality (complete samples), *Biometrika.* 52 (1965) 591, <https://doi.org/10.2307/2333709>.
- [55] T.S. Breusch, A.R. Pagan, A simple test for heteroscedasticity and random coefficient variation, *Econometrica.* 47 (1979) 1287, <https://doi.org/10.2307/1911963>.
- [56] C. Spearman, The proof and measurement of association between two things, *Am. J. Psychol.* (1904), <https://doi.org/10.2307/1412159>.
- [57] C. Cox, J.E. Reeder, R.D. Robinson, S.B. Suppes, L.L. Wheelless, Comparison of frequency distributions in flow cytometry, *Cytometry.* 9 (1988) 291–298, <https://doi.org/10.1002/cyto.990090404>.
- [58] J.T. Cirulis, B.C. Strasser, J.A. Scott, G.M. Ross, Optimization of staining conditions for microalgae with three lipophilic dyes to reduce precipitation and fluorescence variability, *Cytometry Part A* 81 (A) (2012) 618–626, <https://doi.org/10.1002/cyto.a.22066>.
- [59] T.A. Beacham, C. Bradley, D.A. White, P. Bond, S.T. Ali, Lipid productivity and cell wall ultrastructure of six strains of *Nannochloropsis*: implications for biofuel production and downstream processing, *Algal Res.* 6 (2014) 64–69, <https://doi.org/10.1016/j.algal.2014.09.003>.
- [60] B.H.J. Yap, S.A. Crawford, R.R. Dagastine, P.J. Scales, G.J.O. Martin, Nitrogen deprivation of microalgae: effect on cell size, cell wall thickness, cell strength, and resistance to mechanical disruption, *J. Ind. Microbiol. Biotechnol.* 43 (2016) 1671–1680, <https://doi.org/10.1007/s10295-016-1848-1>.
- [61] R. Notman, M. Noro, B. O'Malley, J. Anwar, Molecular basis for dimethylsulfoxide (DMSO) action on lipid membranes, *J. Am. Chem. Soc.* 128 (2006) 13982–13983, <https://doi.org/10.1021/ja063363t>.
- [62] A.A. Gurtovenko, J. Anwar, Modulating the structure and properties of cell membranes: the molecular mechanism of action of dimethyl sulfoxide, *J. Phys. Chem. B* 111 (2007) 10453–10460, <https://doi.org/10.1021/jp073113e>.
- [63] F. He, W. Liu, S. Zheng, L. Zhou, B. Ye, Z. Qi, Ion transport through dimethyl sulfoxide (DMSO) induced transient water pores in cell membranes, *Mol. Membr. Biol.* 29 (2012) 107–113, <https://doi.org/10.3109/09687688.2012.687460>.
- [64] L. Petruš, D.G. Gray, J.N. BeMiller, Homogeneous alkylation of cellulose in lithium chloride/dimethyl sulfoxide solvent with dimethyl sodium activation. A proposal for the mechanism of cellulose dissolution in LiCl/Me₂SO, *Carbohydr. Res.* 268 (1995) 319–323, [https://doi.org/10.1016/0008-6215\(94\)00330-I](https://doi.org/10.1016/0008-6215(94)00330-I).
- [65] A.K. Sum, J.J. De Pablo, Molecular simulation study on the influence of dimethylsulfoxide on the structure of phospholipid bilayers, *Biophys. J.* 85 (2003) 3636–3645, [https://doi.org/10.1016/S0006-3495\(03\)74781-X](https://doi.org/10.1016/S0006-3495(03)74781-X).
- [66] S.E. Broxterman, G. van Erven, H.A. Schols, The solubility of primary plant cell wall polysaccharides in LiCl-DMSO, *Carbohydr. Polym.* 200 (2018) 332–340, <https://doi.org/10.1016/j.carbpol.2018.07.083>.
- [67] M.J. Scholz, T.L. Weiss, R.E. Jinkerson, J. Jing, R. Roth, U. Goodenough, M. C. Posewitz, H.G. Gerken, Ultrastructure and composition of the *Nannochloropsis gaditana* cell wall, *Eukaryot. Cell* 13 (2014) 1450–1464, <https://doi.org/10.1128/EC.00183-14>.
- [68] J.C. Waters, T. Wittmann, Concepts in quantitative fluorescence microscopy, in: *Methods in Cell Biology*, Academic Press Inc., 2014, pp. 1–18, <https://doi.org/10.1016/B978-0-12-420138-5.00001-X>.
- [69] M.A. Rauf, S.S. Ashraf, Radiation Induced Degradation of Dyes-An Overview 166, 2009, pp. 6–16, <https://doi.org/10.1016/j.jhazmat.2008.11.043>.
- [70] C. Le Roy, N. Varin-Blank, F. Ajchenbaum-Cymbalista, R. Letestu, Flow cytometry APC-tandem dyes are degraded through a cell-dependent mechanism, *Cytometry Part A* 75 (2009) 882–890, <https://doi.org/10.1002/cyto.a.20774>.
- [71] L. Kuang, Y. Zhao, W. Zhang, S. Ge, Roles of reactive oxygen species and holes in the photodegradation of cationic and anionic dyes by TiO₂ under UV irradiation, *J. Environ. Eng. (United States)* 142 (2016), [https://doi.org/10.1061/\(ASCE\)EE.1943-7870.0001032](https://doi.org/10.1061/(ASCE)EE.1943-7870.0001032).
- [72] P. Morawski, S. Motley, D. Campbell, Rapid light-dependent degradation of fluorescent dyes in formulated serum-free media, *ImmunoHorizons.* 3 (2019) 585–592, <https://doi.org/10.1101/578856>.
- [73] U. Pick, T. Rachutin-Zalagin, Kinetic anomalies in the interactions of Nile red with microalgae, *J. Microbiol. Methods* 88 (2012) 189–196, <https://doi.org/10.1016/j.mimet.2011.10.008>.
- [74] V. Benito, F. Goñi-de-Cerio, P. Brettes, BODIPY vital staining as a tool for flow cytometric monitoring of intracellular lipid accumulation in *Nannochloropsis gaditana*, *J. Appl. Phycol.* 27 (2014) 233–241, <https://doi.org/10.1007/s10811-014-0310-x>.
- [75] T. Encarnação, C.T. Arranja, T.F.G.G. Cova, A.A.C.C. Pais, M.G. Campos, A.J.F. N. Sobral, H.D. Burrows, Monitoring oil production for biobased feedstock in the microalgae *Nannochloropsis* sp.: a novel method combining the BODIPY BD-C12 fluorescent probe and simple image processing, *J. Appl. Phycol.* 30 (2018) 2273–2285, <https://doi.org/10.1007/s10811-018-1437-y>.
- [76] A. Zienkiewicz, K. Zienkiewicz, E. Poliner, J.A. Pulman, Z.Y. Du, G. Stefano, C. H. Tsai, P. Horn, I. Feussner, E.M. Farre, K.L. Childs, F. Brandizzi, C. Benning, The microalgae *Nannochloropsis* during transition from quiescence to autotrophy in response to nitrogen availability, *Plant Physiol.* 182 (2020) 819–839, <https://doi.org/10.1104/pp.19.00854>.
- [77] J.C. Martin, D.E. Swartzendruber, Time: a new parameter for kinetic measurements in flow cytometry, *Science.* 207 (1980) 199–201, <https://doi.org/10.1126/science.6153131>.
- [78] J.P. Nolan, L.A. Sklar, The Emergence of Flow Cytometry for Sensitive, Real-time Measurements of Molecular Interactions 16, 1998, pp. 633–638, <https://doi.org/10.1038/nbt0798-633>.
- [79] H. Lecoœur, A. Langonné, L. Baux, D. Rebouillat, P. Rustin, M.C. Prévost, C. Brenner, L. Edelman, E. Jacotot, Real-time flow cytometry analysis of permeability transition in isolated mitochondria, *Exp. Cell Res.* 294 (2004) 106–117, <https://doi.org/10.1016/j.yexcr.2003.10.030>.
- [80] H. Pereira, L. Barreira, A. Mozes, C. Florindo, C. Polo, C.V. Duarte, L. Custódio, J. Varela, Microplate-based high throughput screening procedure for the isolation of lipid-rich marine microalgae, *Biotechnol. Biofuels* 4 (2011) 61, <https://doi.org/10.1186/1754-6834-4-61>.
- [81] C.W. Senses, K. Heimann, M. Melkonian, The production of clonal and axenic cultures of microalgae using fluorescence-activated cell sorting, *Eur. J. Phycol.* 28 (1993) 93–97, <https://doi.org/10.1080/09670269300650151>.
- [82] M. Mollet, R. Godoy-Silva, C. Berdugo, J.J. Chalmers, Computer simulations of the energy dissipation rate in a fluorescence-activated cell sorter: implications to cells, *Biotechnol. Bioeng.* 100 (2008) 260–272, <https://doi.org/10.1002/bit.21762>.
- [83] C. Wang, C.Q. Lan, Effects of Shear Stress on Microalgae – A Review 36, 2018, pp. 986–1002, <https://doi.org/10.1016/j.biotechadv.2018.03.001>.
- [84] N.C. Carpita, Tensile Strength of Cell Walls of Living Cells, 1985, <https://doi.org/10.1104/pp.79.2.485>.
- [85] S.J. Lee, B.D. Yoon, H.M. Oh, Rapid method for the determination of lipid from the green alga *Botryococcus braunii*, *Biotechnol. Tech.* 12 (1998) 553–556, <https://doi.org/10.1023/A:1008811716448>.
- [86] G. Bougaran, C. Rouxel, N. Dubois, R. Kaas, S. Grouas, E. Lukomska, J.R. Le Coz, J. P. Cadoret, Enhancement of neutral lipid productivity in the microalgae *Isochrysis affinis Galbana* (T-Iso) by a mutation-selection procedure, *Biotechnol. Bioeng.* 109 (2012) 2737–2745, <https://doi.org/10.1002/bit.24560>.
- [87] M. Isleten-Hosoglu, I. Gultepe, M. Elibol, Optimization of carbon and nitrogen sources for biomass and lipid production by *Chlorella saccharophila* under heterotrophic conditions and development of Nile red fluorescence based method for quantification of its neutral lipid content, *Biochem. Eng. J.* 61 (2012) 11–19, <https://doi.org/10.1016/j.bej.2011.12.001>.
- [88] D. Xu, Z. Gao, F. Li, X. Fan, X. Zhang, N. Ye, S. Mou, C. Liang, D. Li, Detection and quantitation of lipid in the microalgae *Tetraselmis subcordiformis* (Wille) Butcher with BODIPY 505/515 staining, *Bioresour. Technol.* 127 (2013) 386–390, <https://doi.org/10.1016/j.biortech.2012.09.068>.
- [89] M.S. Cooper, W.R. Hardin, T.W. Petersen, R.A. Cattolico, Visualizing “green oil” in live algal cells, *J. Biosci. Bioeng.* 109 (2010) 198–201, <https://doi.org/10.1016/j.jbiosc.2009.08.004>.